



**HAL**  
open science

## **Tropical cyclone Marlene and stratosphere-troposphere exchange**

Jean-Luc Baray, Gérard Ancellet, Tantely Randriambelo, Serge Baldy

► **To cite this version:**

Jean-Luc Baray, Gérard Ancellet, Tantely Randriambelo, Serge Baldy. Tropical cyclone Marlene and stratosphere-troposphere exchange. *Journal of Geophysical Research: Atmospheres*, 1999, 104 (D11), pp.13953 - 13970. <10.1029/1999jd900028>. <hal-04941415>

**HAL Id: hal-04941415**

**<https://hal.science/hal-04941415v1>**

Submitted on 11 Feb 2025

**HAL** is a multi-disciplinary open access archive for the deposit and dissemination of scientific research documents, whether they are published or not. The documents may come from teaching and research institutions in France or abroad, or from public or private research centers.

L'archive ouverte pluridisciplinaire **HAL**, est destinée au dépôt et à la diffusion de documents scientifiques de niveau recherche, publiés ou non, émanant des établissements d'enseignement et de recherche français ou étrangers, des laboratoires publics ou privés.



HAL Authorization

## Tropical cyclone Marlene and stratosphere-troposphere exchange

Jean-Luc Baray

Laboratoire de Physique de l'Atmosphère, Reunion University, St. Denis Message, France

Gérard Ancellet

Service d'Aéronomie, Paris VI University, Paris, France

Tantely Randriambelo and Serge Baldy

Laboratoire de Physique de l'Atmosphère, Reunion University, St. Denis Message, France

**Abstract.** Convective tropical cyclones initiate exchanges of mass and energy between the troposphere and the stratosphere. Recent analyses of ozone and water vapor measurements from Measurements of Ozone by Airbus In-Service Aircraft (MOZAIC) data [Suhre *et al.*, 1997] suggest that stratospheric ozone inputs to the troposphere can occur in the tropics near zones of deep convection. In the present paper, we analyze a case study of spectacular stratosphere-troposphere exchange directly linked to the strong tropical cyclone Marlene, that occurred near Mauritius and Reunion Island on April 1995. The amplitude of the ozone peak (300 ppbv at 300 hPa) is comparable to those observed by Suhre *et al.* In this case, ageostrophic phenomena dominate advective phenomena. Therefore convective effects can be at the origin of mesoscale tropospheric ozone contaminations which affect the entire tropical free troposphere.

### 1. Introduction

Tropospheric ozone studies are of wide interest because of ozone's oxidizing capacity and toxicity. Using satellite data, Fishman *et al.* [1991] observed a widespread seasonal enhancement of ozone over the tropical South Atlantic Ocean during austral spring. Using airborne measurements, other authors identified enhanced ozone air masses coming from different origins in the high troposphere of tropical and equatorial regions of the Atlantic Ocean [Gouget *et al.*, 1996; Suhre *et al.*, 1997]. Since 1992, ozone measurements have been performed regularly in the southwestern region of the Indian Ocean, at Reunion Island [Baldy *et al.*, 1996] and less regularly at Irene in South Africa [Diab *et al.*, 1996]. Multiple mechanisms may be required to explain high ozone concentrations in upper levels of the troposphere in this region. Part of ozone in the upper tropical troposphere comes from the stratosphere by dynamical exchanges linked to subtropical jet-front systems. These dynamic singularities in the upper troposphere have been extensively studied, measured, and modeled in midlatitudes [Reed, 1955; Danielsen, 1968; Reiter, 1975; Shapiro, 1980; Ancellet *et al.*, 1991; Holton *et al.*, 1995], but interest in the subtropical jet stream is relatively new. Recent studies show that the subtropical jet stream can in some cases be the origin of tropopause folds, leading to stratospheric intrusion into the troposphere. Mechanisms are similar to those observed at midlatitudes in relation to the polar jet stream [Gouget *et al.*, 1996; Folkens and Appenzeller, 1996]. A first case study, using total ozone mapping spectrometer (TOMS) and European Centre for Medium-Range Weather Forecasts (ECMWF) data, in the

Indian Ocean region suggested a baroclinically driven stratospheric intrusion into the tropical troposphere between Reunion and Madagascar Islands [Baray *et al.*, 1998a].

Ozone inputs to the troposphere can be also explained by emissions from biomass burning. Seasonality of vegetation fires occur during the August to November period at Madagascar and in the southeastern part of Africa [Randriambelo *et al.*, 1997, 1998]. When a biomass burning zone and a convective zone are close enough in time and space, large quantities of ozone and ozone precursors may be injected into the free troposphere [Chatfield and Delany, 1990]. Under the influence of westerly winds, air masses can be also advected eastward and are expected to contaminate ozone profiles of Reunion Island (which is located approximately 600 km east of Madagascar).

Finally, large tropospheric ozone variability is often directly related to convection mechanisms. Links between ozone and tropical convection have been studied extensively from aircraft measurements of trace chemical species [Pickering *et al.*, 1991; Kriz *et al.* 1993] and from satellite imagery analysis and numerical simulations [Soong and Tao, 1980; Tao and Simpson, 1989; Lafore and Moncrieff, 1989; Pickering *et al.*, 1990; Thompson *et al.*, 1997]. This link between ozone variability and convection was one of the questions addressed by a major field observing program known as the Central Equatorial Pacific Experiment (CEPEX), conducted in March of 1993 [Kley *et al.*, 1993; Lohmann *et al.*, 1995]. Apart from its role in upward transport and diffusion of chemical species produced by biomass burning, the influence of convection upon tropospheric ozone is complex and has both dynamical and chemical aspects. The dynamical removal of ozone by convective clouds has not been rigorously proven, but it has been established that tropical convection reinforces the destruction of ozone and the production of hydroxide radicals by photochemical reactions

Copyright 1999 by the American Geophysical Union.

Paper number 1999JD900028.  
0148-0277/99/1999JD900028\$09.00

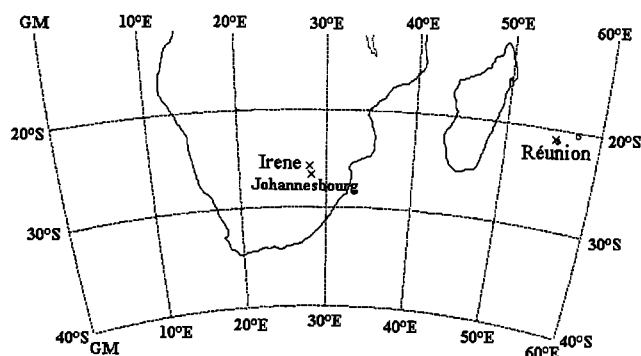


**Figure 1.** Map of the southwestern Indian Ocean region showing the location of the three stations used in this study.

[Logan *et al.*, 1981; Lelieveld and Crutzen, 1990]. Lightning is also thought to contribute significantly to the  $\text{NO}_x$  budget and could lead to the photochemical production of ozone in the free troposphere [Pickering *et al.*, 1993]. From a dynamical point of view, the role of the convection not only includes upward lifting of low ozone air from the PBL, but also the detrainment of air in the upper tropospheric layers could play an important part in the tropospheric ozone budget [Lelieveld and Crutzen, 1994]. The tropical troposphere contains a large quantity of water, and the influence of convective tropical cumulonimbus and cyclones reaches the level of the tropopause in many cases, inducing a weakening of the tropopause [Mitra, 1996]. The tropopause structure near strong convective events is often complex, and exchanges between the stratosphere and the troposphere during these events should occur in both directions (although usually only the transport from the troposphere to the stratosphere is considered). Large ozone peaks (100 to 500 ppbv) associated with tropospheric water vapor mixing ratios ( $0.4$  to  $0.6 \text{ g kg}^{-1}$ ) have been recently identified in the high troposphere of the equatorial Atlantic Ocean from Measurement of Ozone by Airbus In-Service Aircraft (MOZAIC) data. These air masses, rich in ozone and humidity, have been associated with stratosphere-to-troposphere quasi-isentropic transport caused by tropical convection [Suhre *et al.*, 1997; Crutzen and Lawrence, 1997]. The objective of this work is to explore a case study of stratosphere-troposphere exchange directly linked to Marlene, a strong tropical cyclone that occurred near Mauritius and Reunion islands in April 1995. The next part, section 2, describes the data set used in this paper. Section 3 summarizes the climatological characteristics of the region, in order to provide the background values and the meteorological context against which the present study is discussed. Sections 4 and 5 include an analysis of experimental and numerical data for Marlene.

## 2. Data

Three measurement sites, relatively close to each other and located in the same latitude band (between  $20^\circ\text{S}$  and  $25^\circ\text{S}$ , Figure 1) are used to establish the background values of the region of study.

### 2.1. Irene and Reunion Radiosonde Data

Vertical ozone, pressure, and temperature profiles are obtained from radiosondes launched at Irene between June 1990 and August 1993 and from sondes launched at Reunion Island between September 1992 and November 1997. The frequency

of measurement is every 2 weeks at Reunion, giving a total of 86 profiles. At Irene the frequency was weekly, with an increased rate during the Southern African Fire-Atmosphere Research Initiative (SAFARI-92) campaign in September and October 1992. The balloon-borne device used at Irene was a Science Pump, Type 5A electrochemical concentration cell (ECC) ozonesonde, and the corresponding Reunion material was a Vaisala, RS 80-15 PTU sonde in association with an EN-SCI ECC ozonesonde. The accuracy of these devices has been evaluated to 6–10% in the troposphere by field test [Barnes *et al.*, 1985], and the vertical resolution of the data is approximately 50 m.

### 2.2. MOZAIC Data

Aircraft data were used in this study to document climatological ozone, temperature, and humidity distributions (section 3). The MOZAIC program is a European research project which consists of five commercial Airbus A340 aircraft equipped with ozone, temperature, humidity, and wind measuring instruments [Marenco, 1996]. Most of the equipped aircraft fly in Europe and North America, but some measurements occur near the region of present study. In this work, we used measurements in the vicinity of the Johannesburg airport, obtained from aircraft on the Vienna-Johannesburg route (Austrian Airlines). This data set includes 184 profiles (97 landings and 87 takeoffs) between March 1995 and April 1997. The vertical resolution of the MOZAIC data is approximately 150 m during the takeoff and landing phases. The ozone-measuring device is a Dasibi UV absorption thermo-electron model 49-103, the water vapor measurements are obtained from a Vaisala humicap-H, and temperature is derived from a PT100 temperature sensor. All the sensors are located at the front of the plane, to minimize the aircraft's influence on the measurements.

### 2.3. Model Data

The basic medium-range data used in this study are National Centers for Environmental Prediction/National Center for Atmospheric Research (NCEP/NCAR) and ECMWF analyses. Resolution of the analyses is  $2.5^\circ$  in latitude and longitude for 17 vertical levels of pressure between 1000 and 10 hPa for the National Meteorological Center (NMC) model and  $1.125^\circ$  for 15 levels of pressure for the ECMWF model. The time resolution is 6 hours (0, 6, 12, and 18 hours UT).

### 2.4. Satellite Data

Two kinds of satellite images are available in Indian Ocean: geostationary satellite images (Meteosat), and polar orbiting satellite images National Oceanic and Atmospheric Administration-advanced very high resolution radiometer (NOAA-AVHRR). Reunion Island is located near the edge of geostationary observations (Meteosat), while NOAA satellite images offer a wider coverage of the Indian Ocean. Consequently, we use for the present study two types of high-resolution (1 km) satellite images obtained from the NOAA-AVHRR detector. The first, composed of data from several satellite passes, displays the sea surface temperature (SST) [Barton and Cechet, 1989; Barton *et al.*, 1989] and permits detection of cloudy regions (but does not give information on the type of cloud). The second is obtained from only one pass of the satellite and presents the brightness temperature of channel 4 [Kidwell, 1995], and these data represent the cloud top altitude near Reunion Island.

### 3. Background Climatological Profiles

We have calculated climatological profiles for each site using available data to describe four seasonal periods (Figure 2). The December–February period (austral summer) is mainly influenced by convection motions near the Intertropical Convergence Zone (ITCZ). The June–August winter profile is influenced by the proximity of the westerly subtropical jet stream. During the September–November period the spring ozone profile is thought to be mainly influenced by biomass burning emissions in Africa. Tropospheric ozone follows an annual cycle, with minimum ozone mixing ratios in autumn and maximum in spring. This seasonal variation and the average ozone profiles are the same at all the sites. However, the Irene ozonopause (the height where the vertical ozone gradient goes up from a tropospheric value, less than  $5 \text{ ppbv km}^{-1}$ , to a stratospheric value, about  $50 \text{ ppbv km}^{-1}$ ) is systematically about 1 km lower than the Reunion ozonopause. This is probably due to the respective geographical positions of Irene and Reunion. The Irene latitude is  $25^{\circ}\text{S}$ , while the Reunion latitude is  $21^{\circ}\text{S}$ , and so the influence of jet stream is stronger over Irene than Reunion. The fact that the ozonopause is lower than the thermal tropopause (the height where vertical temperature gradient goes up from a tropospheric value, about  $-6^{\circ}\text{C km}^{-1}$ , to a stratospheric value, about  $+3^{\circ}\text{C km}^{-1}$ ) means that there is ozone in the upper tropical troposphere. This factor suggests the permeability of the tropical tropopause, which can arise from ageostrophic circulations near the jet stream (in winter) and from vertical motions in convective system (in summer). This is sometimes observed at midlatitude sites in the northern hemisphere [Bethan *et al.*, 1996], but it is not a quasi-permanent feature as observed at tropical latitude, and the photochemical source is lower than in the northern hemisphere. This observation may support the stratospheric origin of the ozone measured in the 12–16 km region. Temperature profiles are quite similar for the three measurement sites, and the tropopause level is quite constant during the year, between 17 and 18 km height. A maximum in humidity appears during the convective seasons, as expected, from September to February. The humidity profiles extracted from the MOZAIC data give higher values than the radiosoundings, especially in the September–November period. Considering the good agreement between the ozone profiles (less than 20% deviation), a nearly perfect accordance of the temperature profiles (less than 2%) and a more approximate accordance for humidity profiles, we have calculated regional average profiles (averaging the three sites). We will consider these profiles as representative of our region of study: the southwestern part of the Indian Ocean. It should be in addition considered that for humidity, some differences are to be expected between the various sites of measurement.

### 4. Observations of the Case Study

A radiosonde was launched from *St. Denis de la Réunion* on April 6, 1995 (Figure 3). This radiosonde shows very unusual characteristics. Extremely high values of the ozone profile in the whole free troposphere (ozone partial pressure higher than 50 to 80 nbar between the pressure levels 800 and 250 hPa, and an ozone concentration higher than 100 ppbv between 800 and 100 hPa) are observed. These values are largely above those of the average profile calculated for the austral autumn in section 3. In addition to the very high average level of this ozone profile, two peaks are apparent, one at 260 hPa (10.5 km)

above 300 ppbv, and a secondary peak of lower intensity (200 ppbv) at 350 hPa (9 km). The humidity profile is characterized by high values in the low layers (60% below 6 km), yet the two ozone peaks are strongly anticorrelated with humidity. To highlight these characteristics, we have plotted in Figure 4 the difference between the April 6 profile and the climatological background profile calculated in section 3 from MOZAIC data and from Irene and Reunion radiosondes corresponding to the March–May period. In lower layers (1 to 6 km), humidity and ozone are slightly anticorrelated (the slope of the regression line is  $-0.41$ ). For the layers which are strongly enriched in ozone (6 to 14 km), the anticorrelation is much clearer (the slope of the regression line is  $-2.82$ ). The corresponding correlation coefficients ( $-0.36$  and  $-0.48$ ) are significantly different from zero, as indicated by a 98% *t* test. The temperature profile presents a very regular vertical gradient for the whole troposphere, close to the saturated lapse rate ( $-6.5^{\circ}\text{C km}^{-1}$ ). The thermal tropopause is well defined with an abrupt break of the lapse rate at the height 17 km. This temperature profile is consistent with deep convection of the whole troposphere. Wind measurements indicate a weak easterly wind (5 to  $10 \text{ m s}^{-1}$ ) in the lower layers, and a regular rotation of the wind resulting in a westerly wind of slightly higher intensity in the higher layers (over 600 hPa).

To exclude the possibility of ECC sonde measurement error, we carefully checked all the sonde parameters. The airflow rate of the ozone sonde sensor was  $222 \text{ mL min}^{-1}$ , within the usual range. The temperatures of the ozone and PTU sondes presented in Table 1 do not present any anomaly. The stratospheric values of ozone partial pressure (130 nbar) are of the order of magnitude of what one usually observes on Reunion radiosoundings. All these points are a good indication that the sonde sensitivity response is satisfactory. The radiosounding reached the altitude 31 km, which corresponds to the 10 hPa pressure level, well above the maximum of ozone partial pressure level (130 nbar at 25–26 km), so we can calculate the integrated ozone content between the ground and the top of the profile, and we obtain the value 246 Dobson units (DU) ( $1 \text{ DU} = 2.69 \cdot 10^{16} \text{ molecules cm}^{-2}$ ). This value compares well to the integrated contents of ozone measured by the *Système d'Analyse par Observation Zénithale (SAOZ)* spectrometer (251.7 DU on April 6, 1995, Table 2), and the similarity of these integrated values give evidence that the sonde worked properly.

### 5. Analyses, Origins, and Causes

Ozone excess in the troposphere can come from two physical phenomena: photochemical production or transfer of ozone from the stratosphere to the troposphere. Photochemical production is favored when ultraviolet radiation is at a maximum, when ozone precursors ( $\text{NO}_x$ ,  $\text{CH}_4$ ,  $\text{CO}$ , etc.) have been injected into the free troposphere and when moisture values are not too important. Reunion Island is not a very polluted place, and the only significant source of ozone precursors in the free troposphere are the bush fires. The fires influencing Reunion Island occur mainly in Madagascar and in the southeastern part of Africa, but their influence is significant only during southern spring [Baldy *et al.*, 1996]. Moreover, this influence does not exceed a net production of  $5 \text{ ppbv d}^{-1}$  [Taupin, 1998]. Inputs from the stratosphere hence are the only plausible explanation. Yet the elaboration of a mechanism that could explain the observation of very large ozone values in the tropics

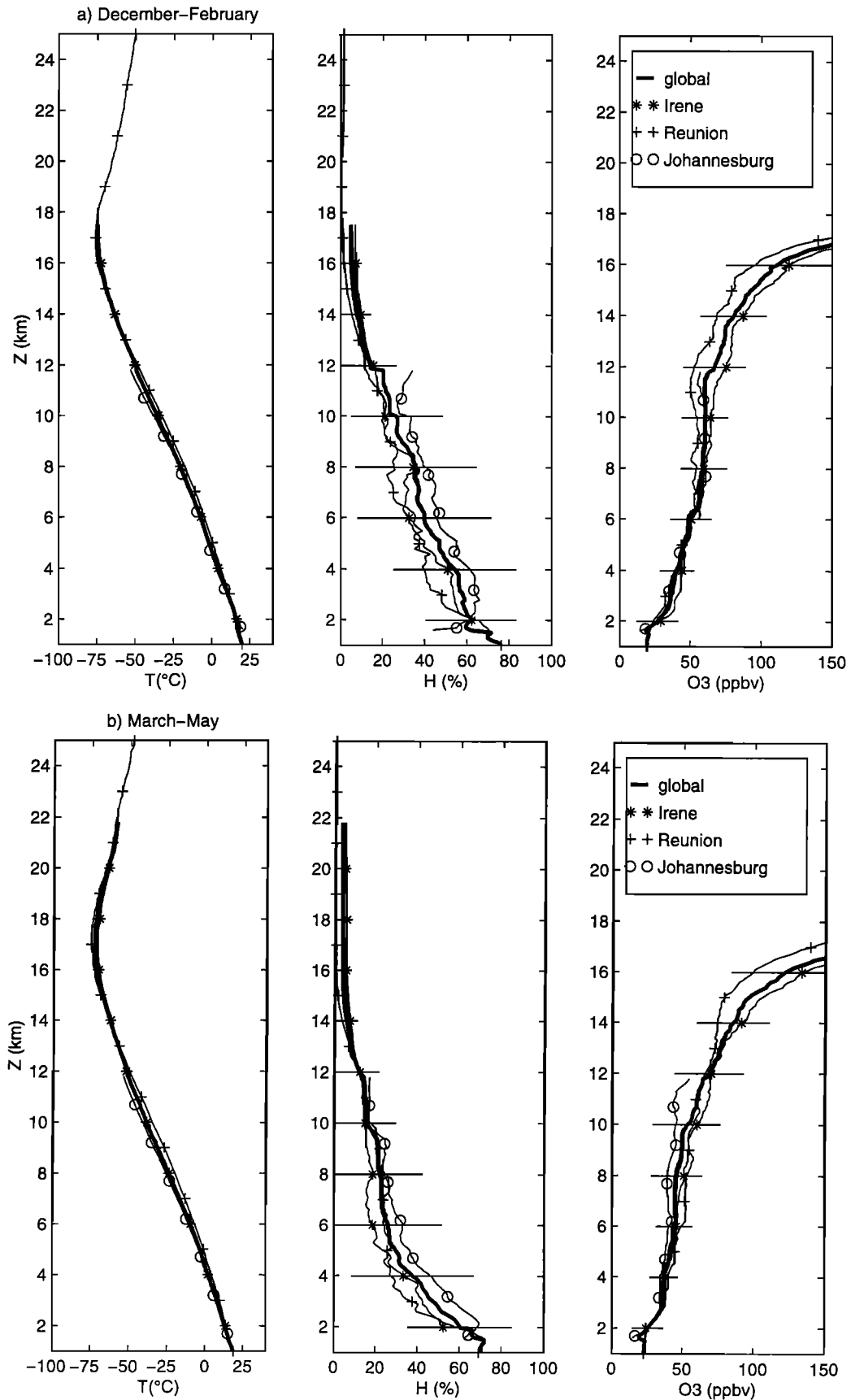


**Figure 2.** Seasonal climatological profiles of temperature, humidity, and ozone concentration over Johannesburg, Reunion, and Irene in (a) austral summer, (b) autumn, (c) winter, and (d) spring. The error bars represent  $\pm 1$  standard deviation calculated on the global profiles.

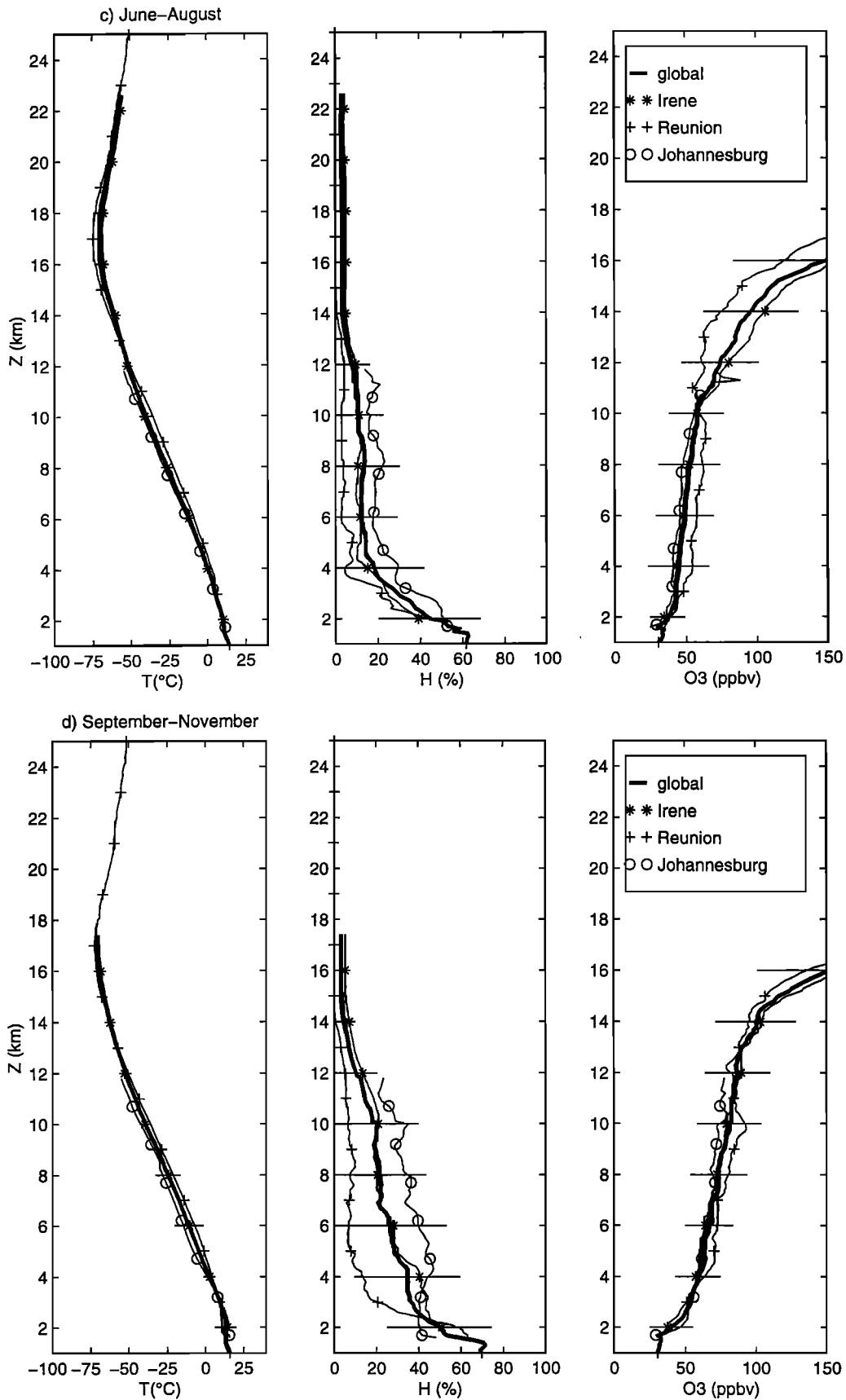
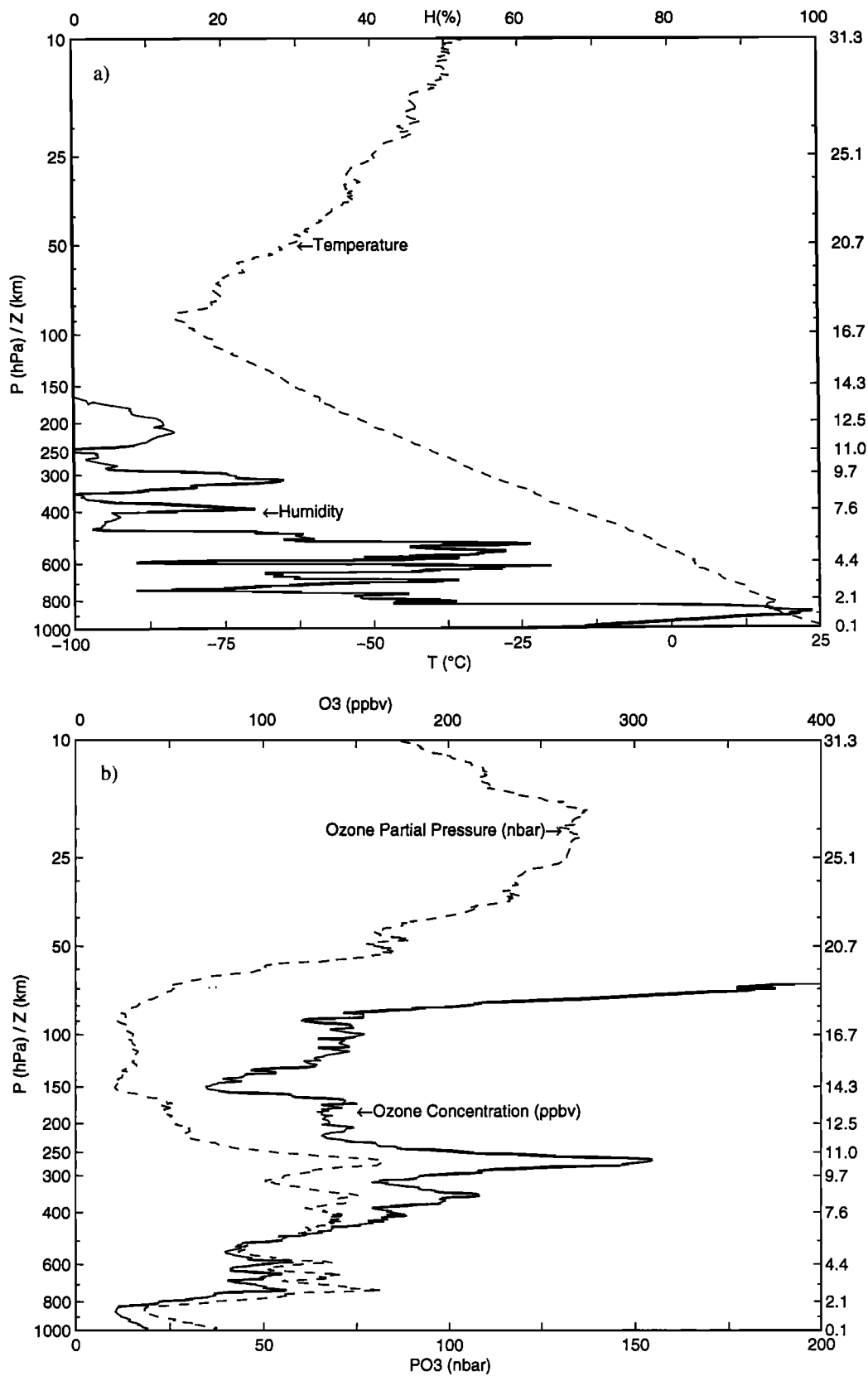


Figure 2. (continued)



**Figure 3.** Profiles of (a) temperature, humidity, (b) ozone partial pressure and concentration, (c) wind, and (d) potential temperature and equivalent saturated potential temperature obtained by radiosounding on April 6, 1995.

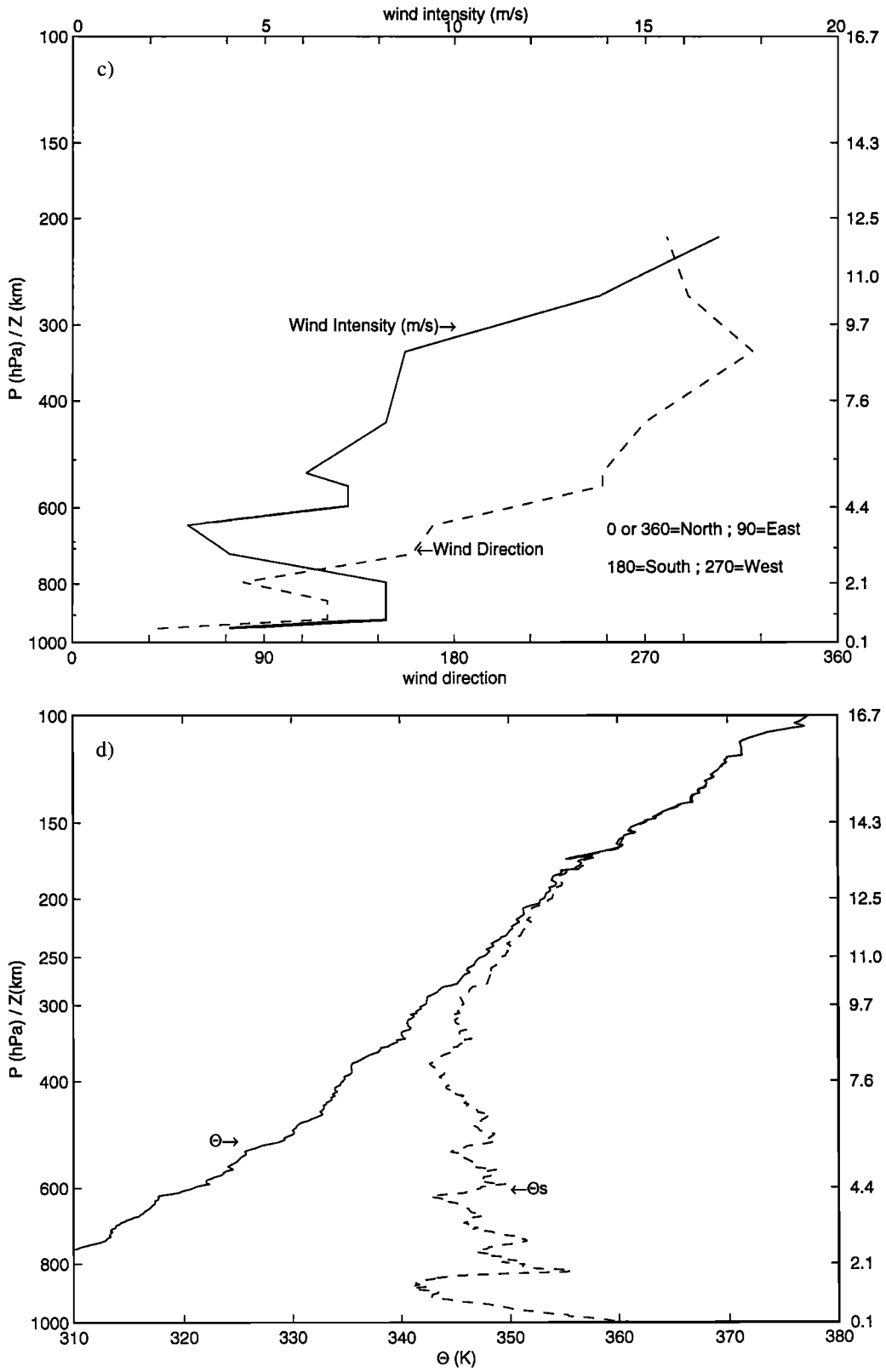
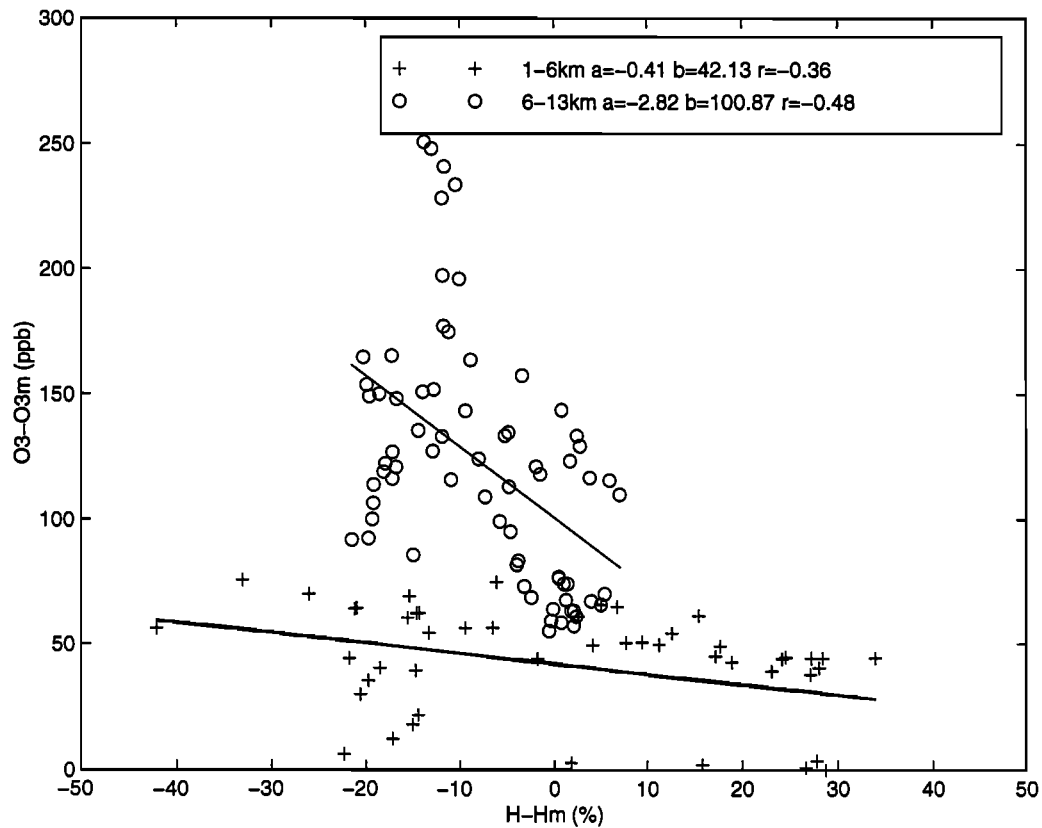


Figure 3. (continued)



**Figure 4.** Scatterplot of  $[O_3]-[O_3]_m$  and  $[H]-[H]_m$ .  $[O_3]$  and  $[H]$  correspond to the April 6 sounding, and  $[O_3]_m$  and  $[H]_m$  are calculated from all the data in the March–May period.

during summer is still pending. Elements for this elaboration are furnished in the following.

The potential temperature and equivalent saturated potential temperature vertical profiles ( $\Theta$  and  $\Theta_s$ , Figure 3d) indicate a stable layer above 300 hPa (9.7 km) and below 300 hPa suggest recent convective activity. The altitude of the ozone peak (7 km below the tropopause, Figure 3b) and the temperature gradient (larger than  $-6.5$  K/km, Figure 3a) support the hypothesis of a relatively stable layer following a deep convective rearrangement. Recent studies showed that the subtropical jet stream could be at the origin of the penetration of stratospheric air to the troposphere via a mechanism similar to the tropopause folds induced by the polar jet stream [Folkins and Appenzeller, 1996; Gouget *et al.*, 1996; Baray *et al.*, 1998a]. Considering the Reunion island latitude ( $21^\circ\text{S}$ ) and the average latitude of the southern subtropical jet stream ( $40^\circ\text{S}$  during

austral summer and  $30^\circ\text{S}$  during austral winter [Hastenrath, 1991]), the ozone peak observed on April 6 is probably not a phenomenon related to the subtropical jet stream. Strong influence of the subtropical jet stream occurs mainly during southern winter, under specific meteorological situations [Baray *et al.*, 1998a]. Both NMC and ECMWF analyses for the first 15 days of April 1995 suggest no strong jet streak effects. Upper level winds on the 300 hPa isobar are weak and located at  $60^\circ\text{E}-80^\circ\text{E}$ ,  $20^\circ\text{S}-30^\circ\text{S}$  for the NMC model and are slightly stronger and located at  $50^\circ\text{E}-65^\circ\text{E}$ ,  $25^\circ\text{S}-30^\circ\text{S}$  for the European model (Figures 5c and 5d). Horizontal wind gradients are not very important; a strong acceleration in the entrance zone and a strong deceleration in the exit zone are not expected. Nevertheless, considering this zone as a jet streak, Reunion Island would be located near the entrance zone, on the anticyclonic face (i.e., the geopotential height of the isobar 300 hPa is over 9.66 km on this side and under 9.56 km on the other

**Table 1.** ECC and PTU Sondes Temperatures

$P$	Ascent		Descent	
	$T_{ptu}$	$T_{ecc}$	$T_{ptu}$	$T_{ecc}$
50	-53.38	16.4	-12.63	26.99
100	-51.73	13.24	-32.11	26.3
150	-38.63	12.4	-46.85	24.8
200	-27.91	13.5	-49.3	23.4
300	-11.53	18.4	-40.8	21.3
400	-0.05	22.5	-28.57	19.9
500	8.462	26.3	-16.83	19.2
600	14.64	29.9	-8.483	19.2
700	20.66	33.3	-0.8299	19.38

**Table 2.** Total Ozone Contents Measured by SAOZ

Date	SAOZ Values, DU
April 1, 1995	251.9
April 2, 1995	247.3
March 4, 1995	249.1
April 4, 1995	250.3
May 4, 1995	249.7
June 4, 1995	251.7
July 4, 1995	243.9
April 8, 1995	246.5

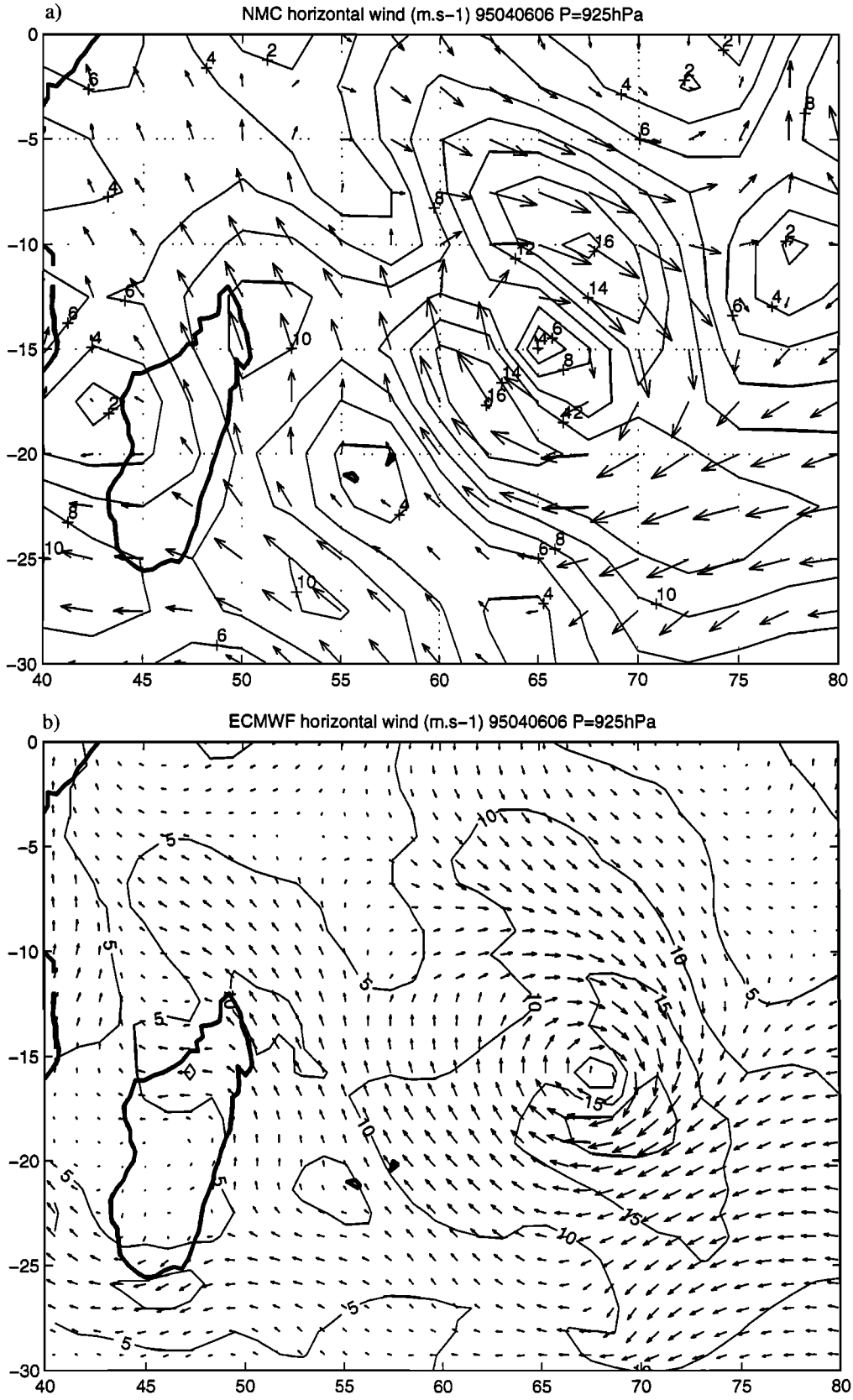


**Figure 5.** NMC and ECMWF horizontal wind on the (a and b) 925 hPa surface and on the (c and d) 300 hPa surface on April 6.

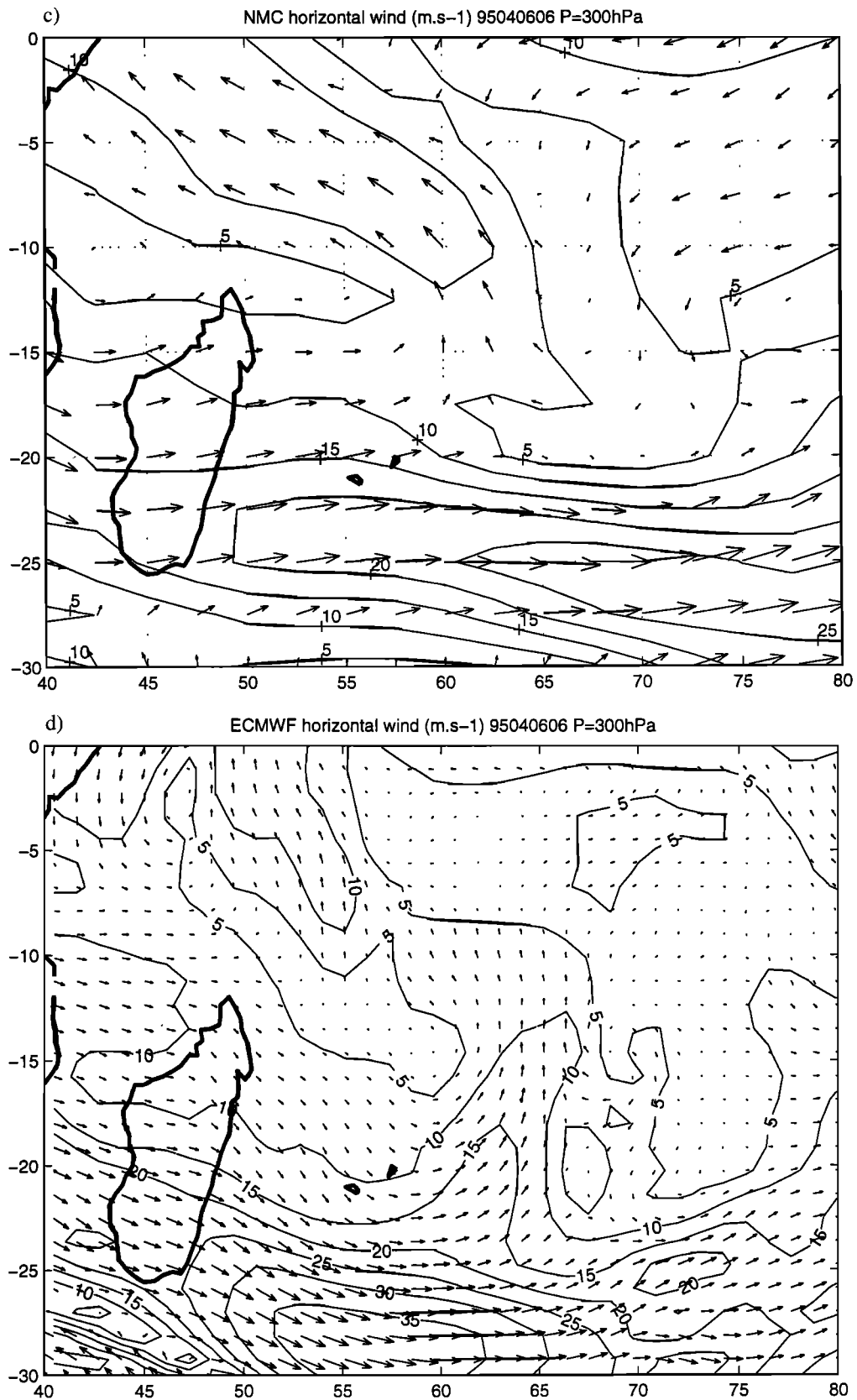


Figure 5. (continued)

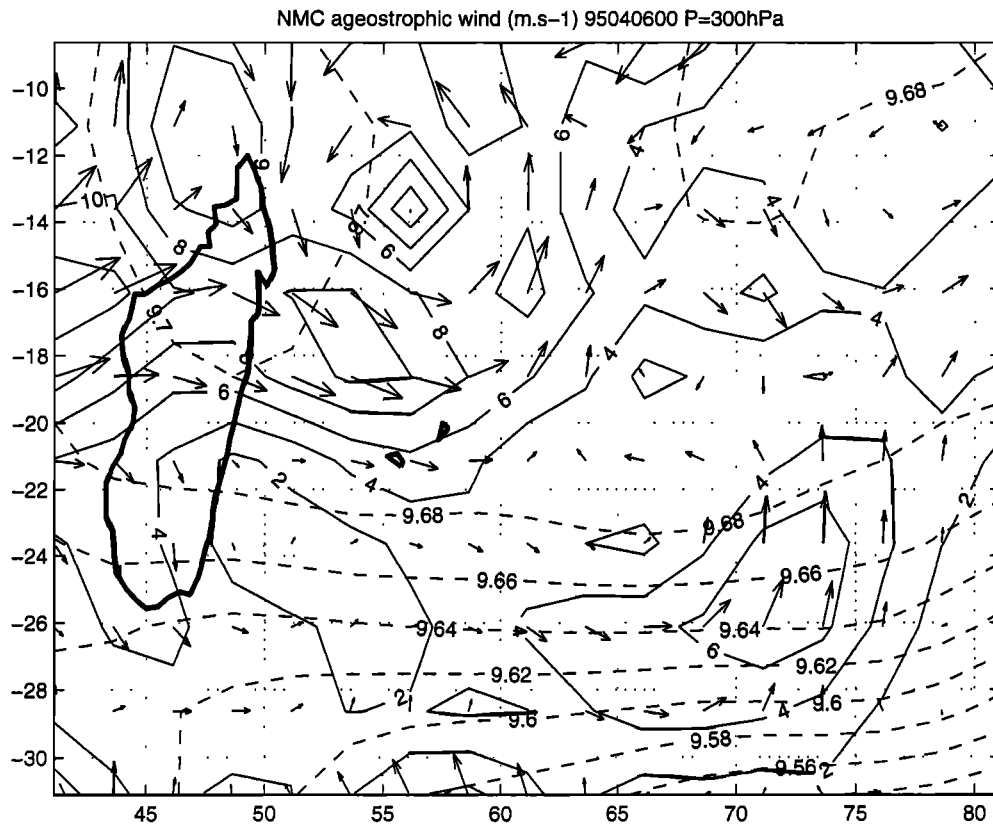


Figure 6. NMC ageostrophic wind and geopotential height on the 300 hPa surface on April 6.

side, Figure 6). However, the probability of a tropopause fold on the anticyclonic side is theoretically weak, and exchanges on this face occur mainly by turbulent flux [Bertin *et al.*, 1995]. This weak jet streak is rectilinear, with a weak intensity ( $25 \text{ m s}^{-1}$ ) in the NMC analyses and a little curved and  $35 \text{ m s}^{-1}$  in the ECMWF analyses. To the contrary, a very strong jet streak associated with a well developed frontogenesis would be needed to explain an ozone peak like that observed on April 6 (Figure 3b), which could only be generated by an extremely significant tropopause fold. Then, the mechanism at the origin of the ozone profile is not likely to be related to the dynamic of the subtropical jet stream.

On the other hand, during this period, the southwestern part of the Indian Ocean was affected by a tropical depression, which was formed on March 30, 1995, about 2000 km northeast of Reunion island. On April 1 it became a tropical cyclone, Marlene, the strongest of the season 1994–1995 in the Indian Ocean [Lander and Angove, 1998]. Between April 3 and 4, Marlene reached a maximum of intensity, with gusts of 160 knots ( $82 \text{ m s}^{-1}$ ) and sustained winds of 130 knots ( $67 \text{ m s}^{-1}$ ). On April 6 its position was at its nearest to Reunion, about 1000 km east. Then Marlene moved away in east-southeast direction while weakening. Meteorological observation data and the trajectory are presented in Figure 7. The satellite images (Plate 1 and Figure 8) enable us to observe the importance of this cyclone and the horizontal area of the associated cloud coverage. The brightness temperature corresponding to this cloud cover is extremely low (less than 200 K). This low value supports the hypothesis of deep convective clouds associated with the cyclone and suggests a cloud development reaching the tropopause. Reunion is not situated in the cloudy

area of the cyclone, but is in its close periphery at around 500 km. In Figure 8 one can observe some low-level convective cloud (280 K) just above Reunion. Upper level clouds (probably cirrus) form a spiral around the most active central part of the cyclone and represent the apparent extension of the upper level divergence associated with the cyclone. These cloud structures, visible on the satellite images, are in agreement with the ageostrophic anticyclonic circulation calculated from the model data (Figure 6).

The cyclone is clearly visible on the NMC data. The cloud zone detected by the satellite images corresponds to cyclonic circulation in the lowest layers (Figures 5a and 5b) and to anticyclonic ageostrophic circulation in the highest layers (Figure 6). Because of the smoothing due to the low resolution of the data, the wind intensity is typically low compared to the observed winds (Figure 7). A modeled wind of  $20 \text{ m s}^{-1}$  corresponds approximately to an observed wind of  $30 \text{ m s}^{-1}$ . The agreement between the vertical structure of the observed wind (Figure 3c) and both model NMC and ECMWF wind is good, with in both cases a southeasterly wind of moderate intensity ( $5$  to  $10 \text{ m s}^{-1}$ ) in the lowest layers, and a westerly wind of higher intensity ( $15$  to  $20 \text{ m s}^{-1}$ ) in the high layers. The wind pattern observed over Reunion (Figure 3c) corresponds to the development of a cyclone in a tropical context. The cyclonic circulation reinforces the southeasterly trade winds usually observed in the lower layers at this location. The wind inversion usually observed in the absence of a cyclone is replaced by a regular rotation of the winds up to the westerly near the tropopause. All these considerations are consistent with the strong apparent influence of cyclonic activity over Reunion. The good agreement between model, satellite, and various observation

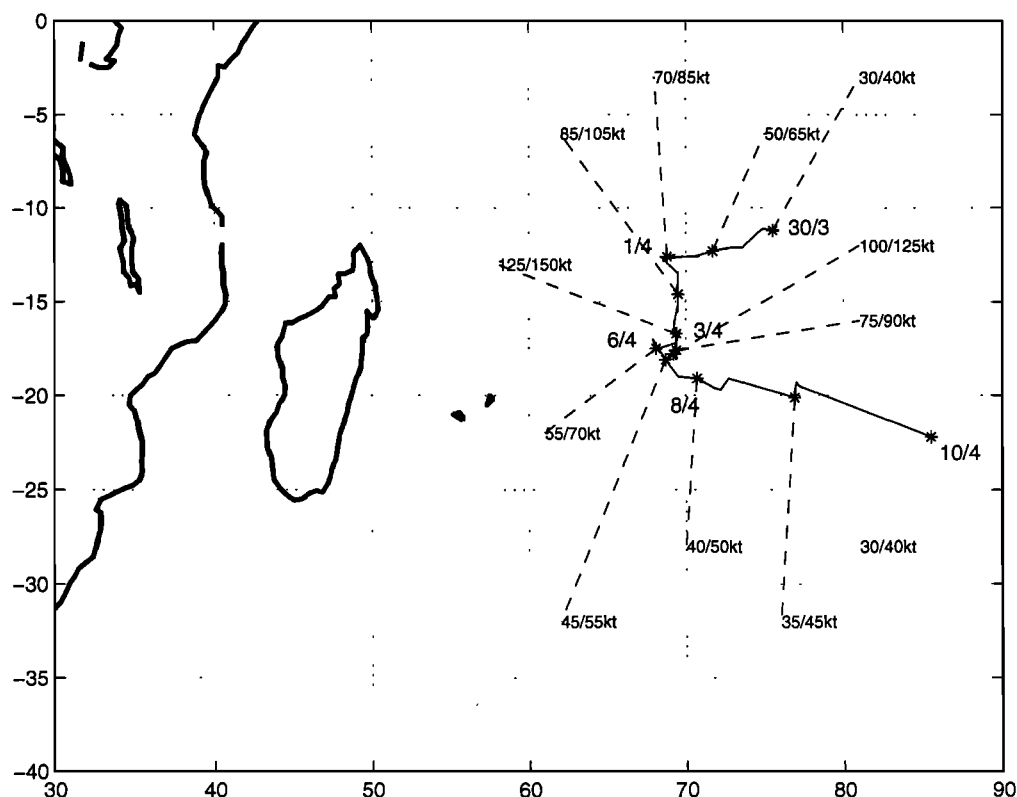


**Figure 7.** Track of the eye of the cyclone Marlene. Maximum sustained wind and gusts in storm are indicated each day, using knot units ( $1 \text{ kt} = 0.51 \text{ m s}^{-1}$ ).

data suggests good validity of the model data. We therefore use NMC and ECMWF data for a qualitative dynamic study.

The most spectacular effect of a tropical cyclone is the generation of violent and destructive winds close to surface. However, the disturbances are not limited to the strong winds close to the surface, since instabilities are also generated over the whole troposphere in the zone of the cyclone and in its proximity. We calculated the potential vorticity (PV), which is a criterion of stability, and is conserved in the atmosphere in the absence of vertical gradients of diabatic heating and friction force [Hoskins *et al.*, 1985]. This is not rigorously the case in the very lower layers, or in the center of the cyclone, but it is roughly true in the periphery. The PV fields on the 225 hPa isobar surface (Figure 9) enable us to notice a dipole structure, characteristic of cyclonic weather circulations [Salby, 1996]. The atmosphere is divided in three zones: a band of high PV values ( $20^{\circ}\text{S}$ ), a band of weak PV ( $20^{\circ}\text{S}$  to  $30^{\circ}\text{S}$ ), and a zone of strong PV below  $30^{\circ}\text{S}$ , corresponding to midlatitudes air masses (Figure 9). The vertical cross sections along the  $21^{\circ}\text{S}$  zonal line (Figure 10) display the vertical structures of the PV anomaly and the vertical wind instabilities. The two models display a rather similar structure, with ascent and strong PV anomalies in the cyclonic zone near  $70^{\circ}\text{E}$ , and with subsidence in the upper troposphere west of the cyclone ( $55^{\circ}\text{E}$ ). Thanks to a better resolution, fine scale PV structures appear more clearly over Reunion Island in the ECMWF cross section (Figure 10b) than in the NMC cross section (Figure 10a). Taking a typical value for vertical velocity of  $0.5 \text{ Pa s}^{-1}$  (Figure 10), one can evaluate the time required for an air mass from 60 hPa level to reach the 300 hPa level. The 60 hPa level corresponds to the stratospheric level where ozone concentrations near 300

ppbv are typically observed, while the 300 hPa level is the altitude of the ozone peak. The resulting transport time of 13 hours is significantly lower than the lifetime of the cyclone (1 week). However, the weak horizontal and vertical resolution of the data makes it difficult to build a more detailed interpretation. To understand the particular structure observed on the ozone profile obtained on April 6, 1995, we calculated the profile of PV over Reunion Island in two ways: first, using only model data, and second, using the relative vorticity from the model and the vertical stability observed by the Reunion radiosonde (Figure 11). Although the NMC model exhibits a tropopause 2 km lower than the ECMWF model, both display the same overall structure for the profile. The layer, which is dry and rich in ozone on the radiosounding (8 to 12 km), corresponds quite well to a relative maximum of PV on the profiles of models, even if the PV values remains less than 2 PVU. The PV profiles are in good agreement with the ozone profile. That indicates that erosion from diabatic phenomena has little time to develop and the air is poorly mixed. The strong enhancement of a large range of ozone profile and the different dynamical elements of this study seem to support the hypothesis of local direct significant downward movements in peripheral regions of intense convective developments. Differential advection from the midlatitude stratospheric reservoir should not play an important role in the observed ozone distribution. It is to be noted that the layer above the ozone peak at the level 150 hPa (Figure 3b) corresponds to the temperature 200 K (Figure 3a); this layer corresponds to the upper level clouds observed on satellite imagery (Figure 8), where some ozone destruction by heterogeneous chemistry should occur [Reichardt *et al.*, 1996]. Lightning can produce  $\text{NO}_x$ , and

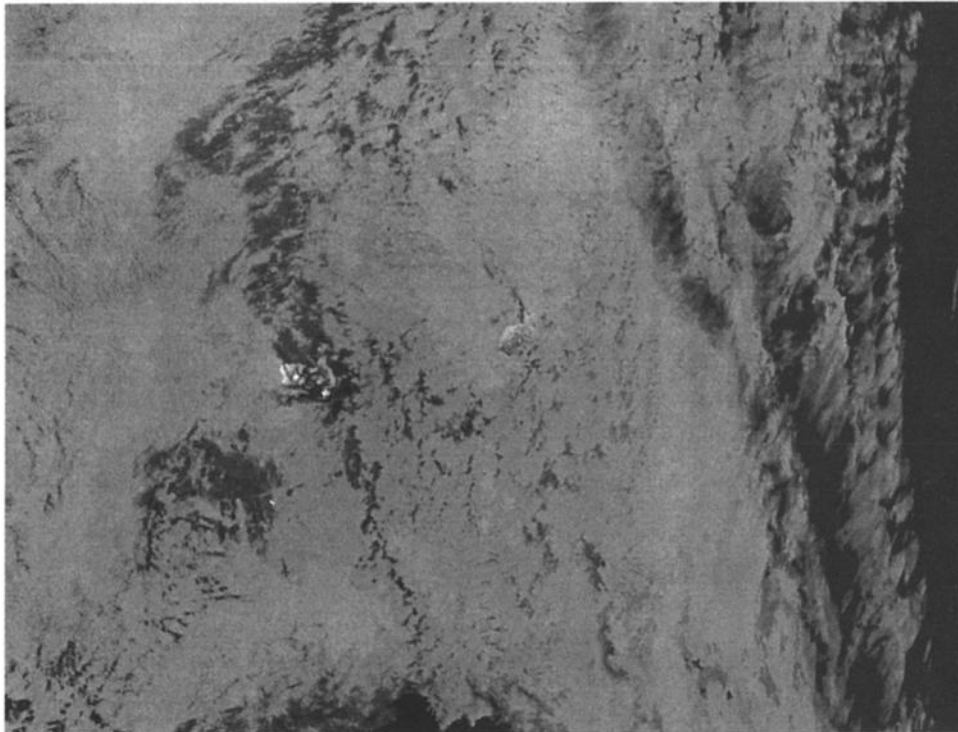


**Figure 8.** Grey level image showing convective clouds in the east of Reunion Island. The image is obtained from the brightness temperature of AVHRR channel 4 at 1034 UT on April 6, 1995. White and black surfaces correspond respectively to cool and warm temperature.

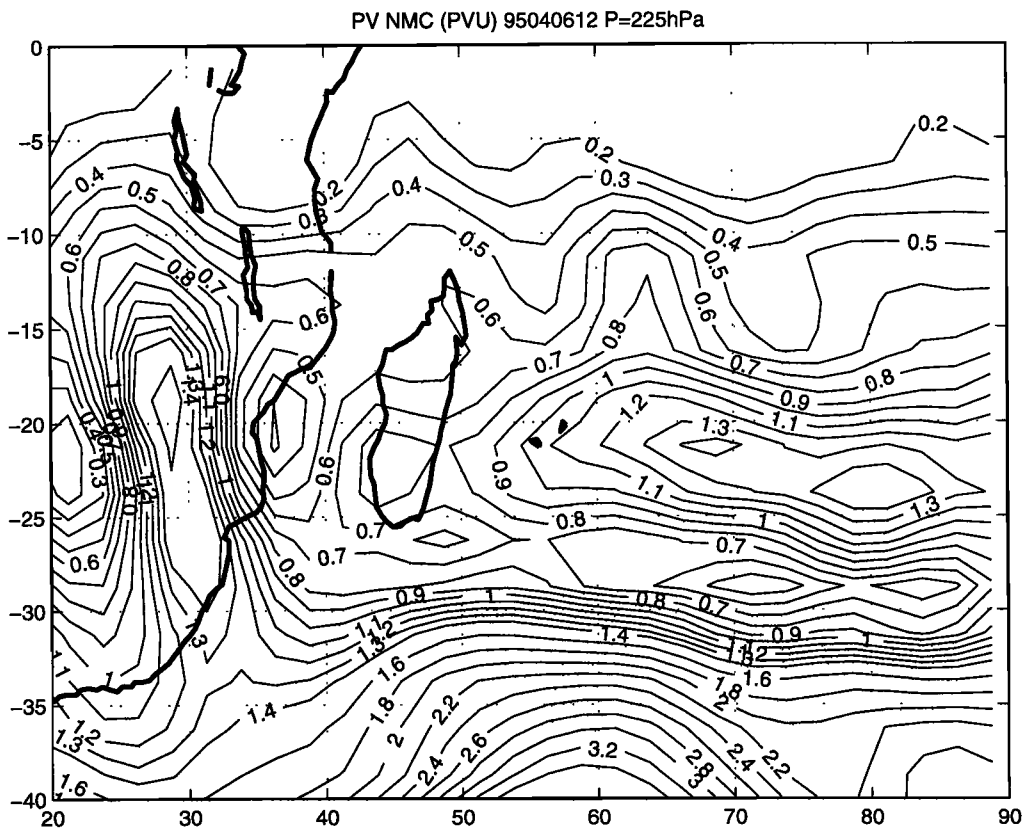


**Figure 9.** Contour map of potential vorticity on April 6, 1995, on the 225 hPa surface. The unit used is the PVU ( $1 \text{ PVU} = 10^{-6} \text{ m}^2 \text{ s}^{-1} \text{ kg}^{-2}$ ).

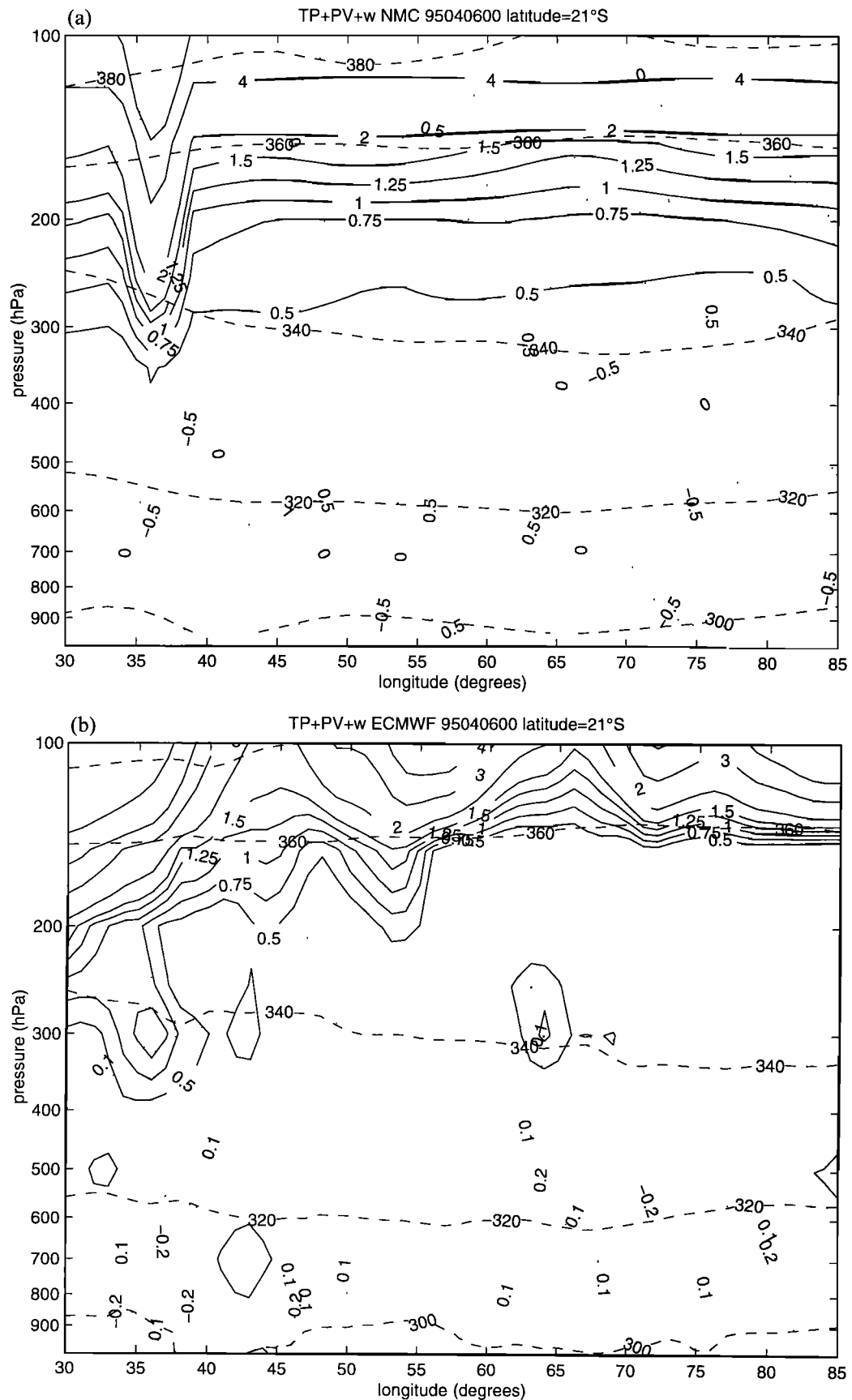


**Figure 10.** (a) NMC and (b) ECMWF zonal (21°S) cross sections showing the potential vorticity (continuous lines), the potential temperature (dashed lines), and the vertical wind component (dotted lines). Negative values of  $w$  indicate ascents, and positive values indicate subsidences.

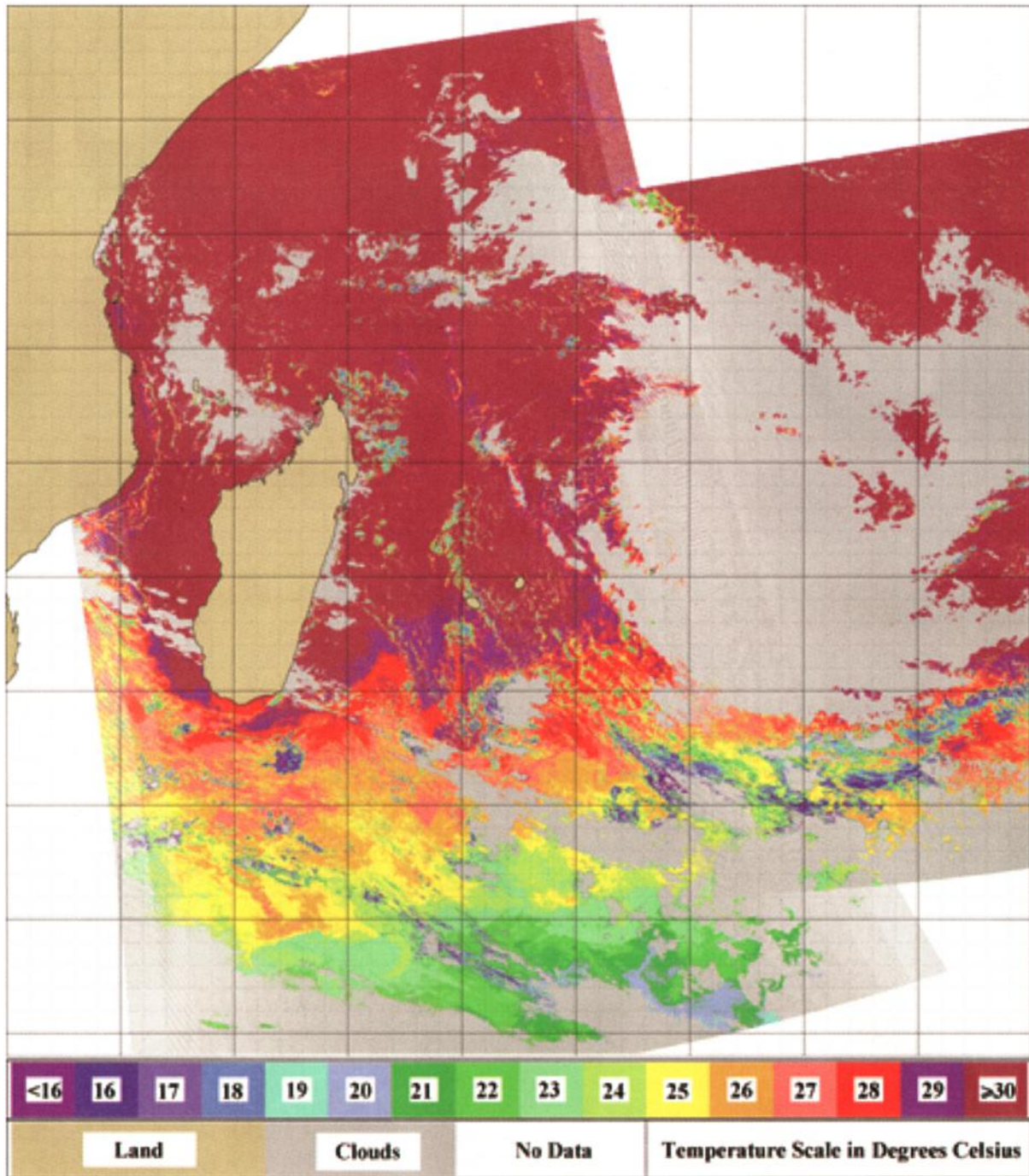


**Plate 1.** False color composite of the sea surface temperature showing convective clouds associated with the cyclone Marlene in the east of Reunion Island. The image is obtained from combining all the satellite crossing over on April 6, 1995.

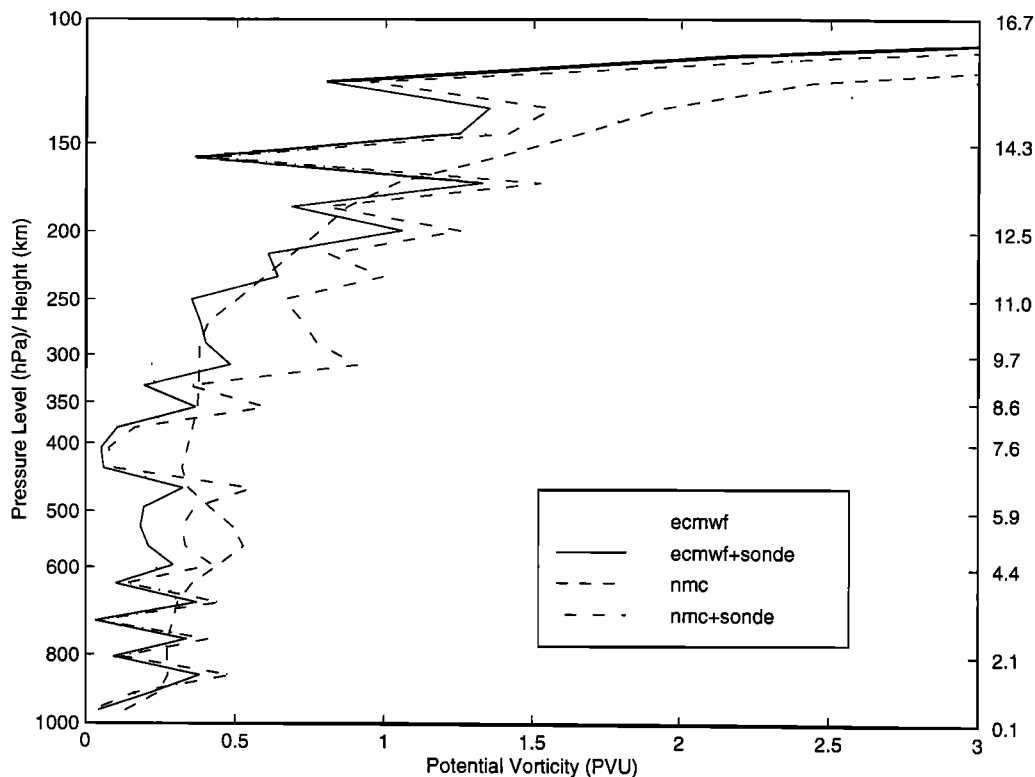


**Figure 11.** Profiles of potential vorticity over Reunion island. Profiles 1 and 3 are calculated directly from model data. Profiles 2 and 4 are obtained by using the vertical stability of the radiosounding and interpolating over 500 m.

then, through photochemistry, influence the ozone budget [Pickering *et al.*, 1993], but that influence is probably not very important. Lightning is dominant over land areas, and it is rarely created by tropical oceanic cyclones like Marlene [Orville and Henderson, 1986; Price and Rind, 1992].

A recent analysis of MOZAIC data made it possible to detect ozone-rich transients (100 to 500 ppbv) in the high troposphere of the equatorial Atlantic [Suhre *et al.*, 1997]. These transients were associated with convective activity, and the authors suggested that transport from the stratosphere toward the troposphere takes place either by direct movement of the air masses or by quasi-isentropic transport. Our study indicates that the first mechanism is more influential. Since these transients were detected during MOZAIC flights, the authors were able to determine the horizontal dimension (about 20 km), but not the vertical extension. The case we analyze in this paper is probably rather similar to that studied by Suhre *et al.*, with transfer to mesoscale generated by a particularly intense convective activity (in our case, a cyclone). The contribution of this study, compared to the study of Suhre *et al.*, is that the radiosonde gives us the vertical distribution of the disturbance that can be generated by a case of convection. This kind of event can, in a specific way, strongly modify a great part of the tropospheric ozone distribution (background values plus 250 ppbv between 10 and 11 km, plus 150 ppbv between 7 and 14 km). These ozone injections of stratospheric origin into the troposphere probably remain too rare to strongly impact the climatological ozone values, but they could explain a part of the small gradient of climatological ozone measured between 10 and 18 km for tropical areas in autumn (Figure 2a). Global-scale models generally do not take into account this

kind of phenomenon and consequently obtain unrealistic climatological profiles for the tropical regions, with near-zero ozone concentrations in the upper tropical troposphere, resulting in a very clear-cut ozonopause [Roelofs *et al.*, 1997].

## 6. Summary and Conclusions

A tropical cyclone is characterized by extremely violent horizontal winds, convergent in the cyclonic direction in the lower layers, divergent in the anticyclonic direction in the high troposphere. By continuity and conservation of mass, secondary vertical circulations are induced (Figure 12). Disturbances in the tropopause above the most active cloud masses can be the origin of transfer from the high troposphere to the low stratosphere. When the cyclone is particularly strong, which was the case for cyclone Marlene, its influence can extend to the outer environment of the cyclone, where mesoscale stratosphere-troposphere transfers are possible. In this article, we observe a perturbation of the ozone profile obtained over Reunion Island, which was in the vicinity of the cyclone. This perturbation is important to almost the whole free troposphere. Our study suggests a direct transport of the mesoscale air masses, induced by strong ageostrophic movements generated in the upper troposphere around the convective area. Model analyses enabled us to detect zones of instability and subsidence above Reunion, although explicit determination of the exchange is not easily visible in the model data which are too diffuse and whose grid is too coarse. Stratosphere-troposphere exchanges linked to midlatitude mesoscale convective complexes (MCC) have been studied with models [Stenchikov *et al.*, 1996] and airplane measurements [Poulida *et al.*, 1996]. These authors

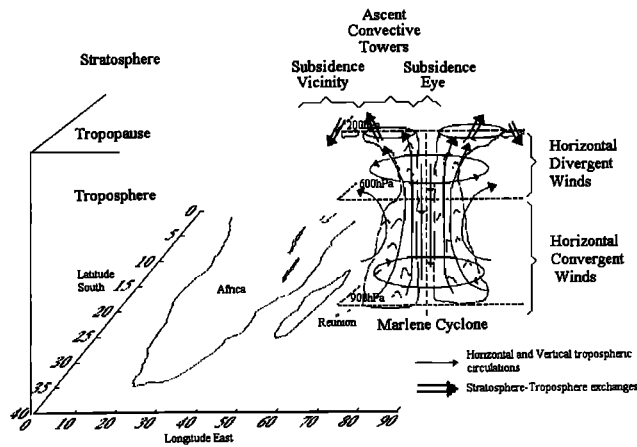


**Figure 12.** Schematic representation showing the circulations generated by the cyclone Marlene.

showed the fine structure of exchanges and contribution on tropospheric ozone. In the case of very strong tropical cyclones, because of the force of the winds, aircraft measurements are more difficult (and very dangerous!).

In our future investigations we plan to supplement these studies by using analyses of mesoscale models (RAMS, mesoNH) and contour advection programs [Waugh and Plumb, 1994; Mariotti et al., 1997] to further determine the effect of isentropic transport and to provide a more refined depiction of interesting phenomena such as subsidence which occurs in the eye of the cyclone. Moreover, new experimental data will allow us to look at the longer-term evolution and frequency of such an observed ozone anomaly. Airborne instrument data will be provided by the Indian Ocean Experiment (INDOEX) campaign in 1999 and a new tropospheric ozone lidar at Reunion operational since June 1998 and will allow tropospheric ozone measurements in clear-sky conditions [Baray et al., 1998b].

**Acknowledgments.** NMC data are provided through CNRS/LMD by courtesy of NCAR/NCEP. The ECMWF is also acknowledged for providing model analyses. Satellite data were extracted from the ORSTOM station of Reunion. The authors wish to acknowledge R. Diab for providing Irene soundings and A. Marengo for providing MOZAIC data. We are also indebted to S. Roumeau and M. Bessafi for helpful discussions, to T. Portafaix for treating SAOZ data, to the radiosounding team of LPA, and finally, to Lee Johnson and the two reviewers whose comments and corrections have contributed to the improvement of the paper.

## References

- Ancellet, G., J. Pelon, M. Beekmann, A. Papayannis, and G. Mégie, Ground-based lidar studies of ozone exchange between the stratosphere and the troposphere, *J. Geophys. Res.*, **96**, 22,401–22,421, 1991.
- Baldy, S., G. Ancellet, M. Bessafi, A. Badr, and D. Lan Sun Luk, Field observation of the vertical distribution of tropospheric ozone at the island of Reunion (southern tropics), *J. Geophys. Res.*, **101**, 23,835–23,849, 1996.
- Baray, J. L., G. Ancellet, F. G. Taupin, M. Bessafi, S. Baldy, and P. Keckhut, Subtropical tropopause break as a possible stratospheric source of ozone in the tropical troposphere, *J. Atmos. Sol. Terr. Phys.*, **60**, 27–36, 1998a.
- Baray, J. L., J. Leveau, J. Porteneuve, G. Ancellet, S. Baldy, and P. Keckhut, Mesures d'ozone troposphérique par sondage lidar à l'île de la Réunion (Océan indien, tropiques sud), livre d'acte de l'atelier expérimentation et instrumentation, pp. 1–2, INSU-Météo-France, Toulouse, France, Dec. 1998b.
- Barnes, R. A., A. R. Bandy, and A. L. Torres, Electrochemical concentration cell ozonesonde accuracy and precision, *J. Geophys. Res.*, **90**, 7881–7887, 1985.
- Barton, I. J., and R. P. Cechet, Comparison and optimization of AVHRR sea surface temperature algorithms, *J. Atmos. Oceanic Technol.*, **6**, 1083–1089, 1989.
- Barton, I. J., A. M. Zavody, D. M. O'Brien, D. R. Cutten, R. W. Saunders, and D. T. Llewellyn-Jones, Theoretical algorithms for satellite-derived sea surface temperatures, *J. Geophys. Res.*, **94**, 3365–3375, 1989.
- Bertin, F., P. Van Velthoven, A. Cremieu, R. Ney, and R. Beugin, UHF radar observation of strato-tropospheric transfers on the anticyclonic side of a jet streak, *Ann. Geophys.*, **13**, 1229–1236, 1995.
- Bethan, S., G. Vaughan, and S. J. Reid, A comparison of ozone and thermal tropopause heights and the impact of tropopause definition on quantifying the ozone content of the troposphere, *Q. J. R. Meteorol. Soc.*, **122**, 929–944, 1996.
- Chatfield, R. B., and A. C. Delany, Convection link biomass burning to increase tropical ozone: However, models will tend to overpredict  $O_3$ , *J. Geophys. Res.*, **95**, 18,473–18,488, 1990.
- Crutzen, P., and M. Lawrence, Ozone clouds over the Atlantic, *Nature*, **388**, 625–626, 1997.
- Danielsen, E. F., Stratospheric tropospheric exchange based on radioactivity, ozone and potential vorticity, *J. Atmos. Sci.*, **25**, 502–518, 1968.
- Diab, R. D., A. M. Thompson, M. Zunckel, G. J. R. Coetzee, J. Combrink, G. E. Bodeker, J. Fishman, D. P. McNamara, C. B. Archer, and D. Nganga, Vertical ozone distribution over southern Africa and adjacent oceans during Safari-92, *J. Geophys. Res.*, **101**, 23,823–23,833, 1996.
- Fishman, J., K. Fakhruzzaman, B. Cros, and D. Nganga, Identification of widespread pollution in the southern hemisphere deduced from satellite analyses, *Science*, **252**, 1693–1696, 1991.
- Folkens, I., and C. Appenzeller, Ozone and potential vorticity at the subtropical tropopause break, *J. Geophys. Res.*, **101**, 18,787–18,792, 1996.
- Gouget, H., J. P. Cammas, A. Marengo, R. Rosset, and I. Jonquière, Ozone peaks associated with a subtropical tropopause fold and with the trade wind inversion: A case study from the airborne campaign TROPOZ II over the Caribbean in winter, *J. Geophys. Res.*, **101**, 25,979–25,993, 1996.
- Hastenrath, S., *Climate Dynamics of the Tropics*, Kluwer Acad., Norwell, Mass., 1991.
- Holton, J. R., P. H. Haynes, M. E. McIntyre, A. R. Douglass, R. B. Rood, and L. Pfister, Stratosphere troposphere exchange, *Rev. Geophys.*, **33**, 403–439, 1995.
- Kidwell, K. B., NOAA Polar Orbiter data user's guide, Natl. Oceanic and Atmos. Admin., Silver Spring, Md., 1995.
- Kley, D. H., H. Voemel, H. Grassl, V. Ramanathan, S. Sherwood, and S. F. Williams, Cross section of tropospheric water vapor during CEPEX between 160°E and 160°W, *Eos Trans. AGU*, **74**(43), Fall Meet. Suppl., 115, 1993.
- Kritz, M. A., S. W. Rosner, K. K. Kelly, M. Loewenstein, and K. R. Chan, Radon measurements in the lower tropical troposphere: Evidence for rapid vertical transport and dehydration of tropospheric air, *J. Geophys. Res.*, **98**, 8725–8736, 1993.
- Lafare, J. P., and M. W. Moncrieff, A numerical investigation of the organization and interaction of convective and stratiform regions of tropical squall lines, *J. Atmos. Sci.*, **46**, 521–544, 1989.
- Lander, M. A., and M. D. Angove, Eastern hemisphere tropical cyclones of 1995, *Mon. Weather Rev.*, **126**, 257–280, 1998.
- Lelieveld, J., and P. Crutzen, Influences of clouds photochemical processes on tropospheric ozone, *Nature*, **343**, 227–233, 1990.
- Lelieveld, J., and P. Crutzen, Role of deep cloud convection in the ozone budget of the troposphere, *Science*, **264**, 1759–1761, 1994.
- Logan, J. A., M. J. Prather, S. C. Wofsy, and M. B. McElroy, Tropospheric chemistry: A global perspective, *J. Geophys. Res.*, **86**, 7210–7254, 1981.
- Lohmann, U., E. Roeckner, W. D. Collins, A. J. Heymsfield, G. M. McFarquhar, and T. P. Barnett, The role of water vapor and convection during the Central Equatorial Pacific Experiment from observations and model simulations, *J. Geophys. Res.*, **100**, 26,229–26,245, 1995.
- Marengo, A., Measurement of Ozone by Airbus In-Service Aircraft (MOZAIC I), technical report, Lab. d'Aérol., Toulouse, France, 1996.

- Mariotti, A., M. Moustouai, B. Legras, and H. Teitelbaum, Comparison between vertical ozone soundings and reconstructed potential vorticity maps by contour advection with surgery, *J. Geophys. Res.*, **102**, 6131–6142, 1997.
- Mitra, A. P., Troposphere-stratosphere coupling and exchange at low latitude, *Adv. Space Phys.*, **17**, 1189–1197, 1996.
- Orville, R. E., and R. W. Henderson, Global distribution of midnight lightning: September 1977 to August 1978, *Mon. Weather Rev.*, **114**, 2640–2653, 1986.
- Pickering, K. E., A. M. Thompson, R. R. Dickerson, W. T. Luke, D. P. McNamara, J. P. Greenberg, and P. R. Zimmerman, Model calculations of tropospheric ozone production potential following observed convective events, *J. Geophys. Res.*, **95**, 14,049–14,062, 1990.
- Pickering, K. E., A. M. Thompson, J. R. Scala, W. K. Tao, J. Simpson, and M. Garstang, Photochemical ozone production in tropical squall line convection during NASA Global Tropospheric Experiment/Amazon Boundary Layer Experiment 2A, *J. Geophys. Res.*, **96**, 3099–3114, 1991.
- Pickering, K. E., A. M. Thompson, W. K. Tao, and T. L. Kucsera, Upper tropospheric ozone production following mesoscale convection during STEP/EMEX, *J. Geophys. Res.*, **98**, 8737–8749, 1993.
- Poulida, O., R. R. Dickerson, and A. Heymsfield, Stratosphere-troposphere exchange in a midlatitude mesoscale convective complex, 1, Observations, *J. Geophys. Res.*, **101**, 6823–6836, 1996.
- Price, C., and D. Rind, A simple lightning parameterization for calculating global lightning distributions, *J. Geophys. Res.*, **97**, 9919–9933, 1992.
- Randriambelo, T., M. Bessafi, and S. Baldy, Deep convection cloud detection using NOAA satellite: Applications to convection transport of biomass burning emissions over southeastern Africa and Madagascar, paper presented at the 1997 EUMETSAT Meteorological Satellite Data User's Conference, Eur. Org. for the Exploit. of Meteorol. Satell., Sept.–Oct. 1997, Brussels, Belgium, 1997.
- Randriambelo, T., S. Baldy, M. Bessafi, M. Petit, and M. Despinov, An improved detection and characterization of active fires and smoke plumes in southeastern Africa and Madagascar, *Int. J. Remote Sens.*, **23**, 2623–2638, 1998.
- Reed, R. J., A study of characteristic type of upper level frontogenesis, *J. Meteorol.*, **12**, 226–237, 1955.
- Reichardt, J., A. Ansmann, M. Serwazi, C. Weitkamp, and W. Michaelis, Unexpectedly low ozone concentration in midlatitude tropospheric ice clouds: A case study, *Geophys. Res. Lett.*, **23**, 1929–1932, 1996.
- Reiter, E. R., Stratospheric-tropospheric exchange process, *Rev. Geophys.*, **13**, 459–474, 1975.
- Roelofs, G. J., J. Lelieveld, H. G. J. Smit, and D. Kley, Ozone production and transports in the tropical Atlantic regions during the biomass burning season, *J. Geophys. Res.*, **102**, 10,637–10,651, 1997.
- Salby, M. L., *Fundamental of Atmospheric Physics*, Academic, San Diego, Calif., 1996.
- Shapiro, M. A., Turbulent mixing within tropopause folds as a mechanism for the exchange of chemical constituents between the stratosphere and troposphere, *J. Atmos. Sci.*, **37**, 994–1004, 1980.
- Soong, S. T., and W. K. Tao, Response of deep tropical clouds to mesoscale processes, *J. Atmos. Sci.*, **37**, 2035–2050, 1980.
- Stenchikov, G., R. Dickerson, K. Pickering, W. Ellis Jr., B. Doddridge, S. Kondragunta, O. Poulida, J. Scala, and W. K. Tao, Stratosphere-troposphere exchange in a midlatitude mesoscale convective complex, 2, Numerical simulations, *J. Geophys. Res.*, **101**, 6837–6851, 1996.
- Suhre, K., J. P. Cammas, P. Nédelec, R. Rosset, A. Marengo, and H. G. J. Smit, Ozone-rich transients in the upper equatorial Atlantic troposphere, *Nature*, **388**, 661–663, 1997.
- Tao, W. K., and J. Simpson, Modeling study of a tropical squall-type convective line, *J. Atmos. Sci.*, **46**, 177–202, 1989.
- Taupin, F., Analyse et modélisation de la variabilité de l'ozone troposphérique en zone tropicale—Influence du brûlage de biomasse, doctoral thesis, Univ. of Clermont II, Aubière, France, 1998.
- Thompson, A. M., W. K. Tao, K. E. Pickering, J. R. Scala, and J. Simpson, Tropical deep convection and ozone formation, *Bull. Am. Meteorol. Soc.*, **78**, 1043–1054, 1997.
- Vonnegut, B., Comment on “Stratosphere-troposphere exchange in a midlatitude mesoscale convective complex, 1, Observations” by O. Poulida et al. and “Stratosphere-troposphere exchange in a midlatitude mesoscale convective complex, 2, Numerical simulations” by G. Stenchikov et al., *J. Geophys. Res.*, **102**, 23,587–23,588, 1997.
- Waugh, D. W., and R. A. Plumb, Contour advection with surgery: A technique for investigating finescale structure in tracer transport, *J. Atmos. Sci.*, **51**, 530–540, 1994.

G. Ancellet, Service d'Aéronomie, Tour 15-14 e5, Paris VI University, 4 place Jussieu, 75252 Paris Cedex 5, France.

S. Baldy, J.-L. Baray, and T. Randriambelo, Laboratoire de Physique de l'Atmosphère, Reunion University, 15 avenue René Cassin, 97715 St. Denis Message Cedex 9, France. (barray@univ-reunion.fr)

(Received August 17, 1998; revised January 13, 1999; accepted January 19, 1999.)